Repair and Retrofit of Concrete Columns with Fiber Composites

Mohammad R. Ehsani, Ph.D., P.E.
Department of Civil Engineering and Engineering Mechanics
University of Arizona
Tucson, AZ 85721

Archive of SID

ABSTRACT

Fiber composite materials have been used for decades in certain industries such as aerospace, ship-building, sporting goods, etc. However, their application in civil engineering structures has received attention only in the recent years. The major advantage of fiber composites is their high tensile strength to weight ratio. Reinforced concrete columns constructed prior to mid 1970s usually have few ties; this lack of confinement results in various brittle modes of failure when the structure is subjected to lateral loads, e.g. during an earthquake. This paper presents the results of several reduced-scale column specimens that were constructed and retrofit by wrapping them with bands of glass fiber composites. The specimens were subjected to simulated earthquake type loading. The results indicate that this technique can be used very effectively in upgrading deficient columns in existing structures. A procedure is also presented to calculate the required thickness of composite materials to ensure a desired level of ductility in the column.

INTRODUCTION

Recent earthquakes have highlighted the shortcomings of older design practices as it relates to reinforced concrete columns. There are primarily two major design deficiencies with the columns constructed prior to mid 1970s when the design codes were changed. The first problem is lack of adequate confinement steel; earlier codes called for 13-mm diameter ties to be placed at a spacing of 300 mm along the column height. This was independent of the column cross section and the number and size of the longitudinal bars. In the event of an earthquake, shortly after the cover or shell portion of the column cracks, the sparsely-spaced ties cannot provide sufficient confinement for the longitudinal bars and they buckle, leading to the collapse of the column. As shown in Fig. 1, while spirally reinforced columns that are well confined suffer minor damage, tied columns with little lateral confinement collapse under severe earthquake loading.

The second problem is the poor detailing used for starter bars. Before the codes were revised in mid 1970s, the practice was to extend the starter bars a length equal to twenty times the bar diameter above the footing; the column longitudinal bars would be lap spliced over that length above the footing. The short lap length combined with insufficient lateral ties prevents the columns to develop their full moment capacity at the base.

www.SID.ir

Both of these problems can be overcome by providing external confinement for the columns. Since the late 1980s it has been shown that encasing existing columns in steel jackets can increase the strength and ductility of such columns significantly [1] and the technique has been extensively used in the U.S. to retrofit a large number of highway bridge piers. It is well recognized that when concrete is confined, its compressive strength and failure strain increase significantly. Figure 2 shows an example of this improvement. The graph in thinner line shows the behavior of a typical unconfined concrete cylinder tested in compression; the specimen fails at a strain of roughly 0.003 shortly after reaching its maximum stress. The behavior of a confined cylinder is shown in the heavier line. Not only the strength of the cylinder is higher, but more importantly the failure strain is increased significantly. The increase in strength and failure strain depends on the amount of confinement provided [2].

Fig. 1. Earthquake damage to a well-confined column and collapse of a poorly-confined column.

Fiber Composites

In recent years, the application of Fiber Reinforced Polymers (FRP) has increased significantly. These materials have high tensile strength to weight ratios. Their flexibility allows them to be wrapped around column sections with different geometries. The light weight of FRPs makes the handling and field construction much easier compared to steel jackets. FRPs consist of very thin fibers that are embedded in a resin. The most common fibers are glass and carbon whose tensile strengths range around 2300 to 2800 MPa. Common resins are polyesters, vinyl esters, and epoxies. The resins do not have much strength but they provide protection for the fibers and cause the load to be uniformly distributed among fibers. The stress-strain behavior of FRPs is linear to failure. More detailed properties of the FRPs used in these studies are provided in the following sections.

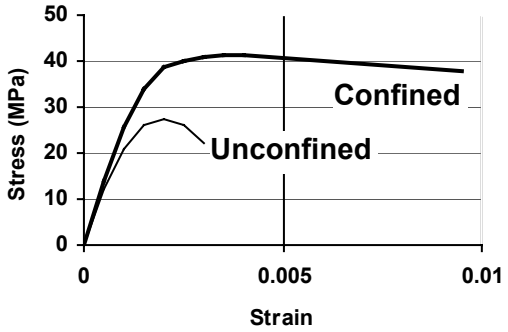

Fig. 2. Stress-strain relationship for confined and unconfined concrete.

Archive of SID

www.SID.ir

EXPERIMENTAL PROGRAM

Test Specimens

Ten specimens were constructed and tested. In addition, four of the specimens were repaired after the initial tests and then retested, resulting in a total of 14 tests (Table 1). The specimens were 1/5 scale models of the prototype bridge piers constructed in California. The test specimens were designed to model typical pre-1971 design of existing highway bridges in a zone of high seismic risk and emphasized two problems with such structures: (1) inadequate starter bar lap length, and (2) insufficient transverse reinforcement. The columns were 1.6 m high and included a square footing that was 40 cm thick. The top end of the columns included a solid concrete cube that was needed to apply the loads to the column; this resulted in the total height for the specimens to be 2.41 m (Fig. 3)

Table 1. Details of Test Specimens

Specimen	f'_C (MPa)	Longitudinal Steel Detail	Retrofit Scheme	No. of Layers	Calculated Strength (MPa)	Measured Max. V_u (MPa)	% Increase due to Retrofit
C1	36.5	Starter	---	---	50.7	58.3	---
C2	38.3	Starter	Passive	6	50.7	81.4	40%
C3	38.5	Starter	Active	6	50.7	89.4	53%
C4	36.6	Continuous	---	---	50.7	71.6	---
C5	36.5	Continuous	Passive	6	50.7	87.2	22%
R1	34.9	Starter	---	---	102.7	96.5	---
R2	33.4	Starter	Active	8	102.7	138.8	44%
R3	33.3	Continuous	---	---	132.5	161.5	---
R4	35.6	Continuous	Passive	8	132.5	214.0	32%
R5	36.2	Continuous	Passive-Oval	8	132.5	226.8	40%
C1R	36.5	Starter	Active	6	58.3*	72.5	24%
C4R	38.3	Continuous	Active	6	71.6*	72.5	1%
R1R	34.9	Starter	Active	8	96.5*	128.5	33%
R3R	33.4	Continuous	Active	8	161.5*	211.3	31%

*Measured values from earlier tests of non-retrofit specimens.

The specimens were divided in two groups, Circular (C) and Rectangular (R). The diameter of the circular columns was 305 mm and the columns were reinforced longitudinally with fourteen 13-mm bars, resulting in a longitudinal reinforcement ratio of 2.48%. Transverse reinforcement was provided in the form of steel wire hoops with a diameter of 3.5 mm spaced at 89 mm along the height of the column. For columns C1, C2, and C3 starter bars extended a distance of 20 bar diameters, i.e. 255 mm, above the top of the footing and were lapped with the column longitudinal steel. For specimens C3 and C4, the column bars were directly anchored into the footing with standard 90-degree hooks.

The rectangular columns had a cross section of 241 mm x 368 mm. Columns R1 and R2 were reinforced longitudinally with twelve 16-mm bars that were lapped to starter bars extending above the footing; this resulted in a longitudinal reinforcement ratio of 2.70%. Columns R3, R4, and R5

Archive of SID

www.SID.ir

were reinforced longitudinally with ten 16-mm bars and twenty two 13-mm bars that were directly anchored into the footing; the reinforcement ratio for these columns was 5.45%.

Material Properties

The measured yield strength for the16-mm, 13-mm and 3.5-mm steel bars were 359 MPa, 358 MPa, and 301 MPa, respectively. Although the concrete compressive strength for the prototype bridge was 21 MPa, a ready-mixed concrete providing f'_c = 35 MPa was used to account for the effect of expected over-strength due to conservative initial mix design and strength gain with concrete aging. The compressive strength of concrete on the day of testing was measured as the average of three cylinders tested to failure and those values are listed in Table 1.

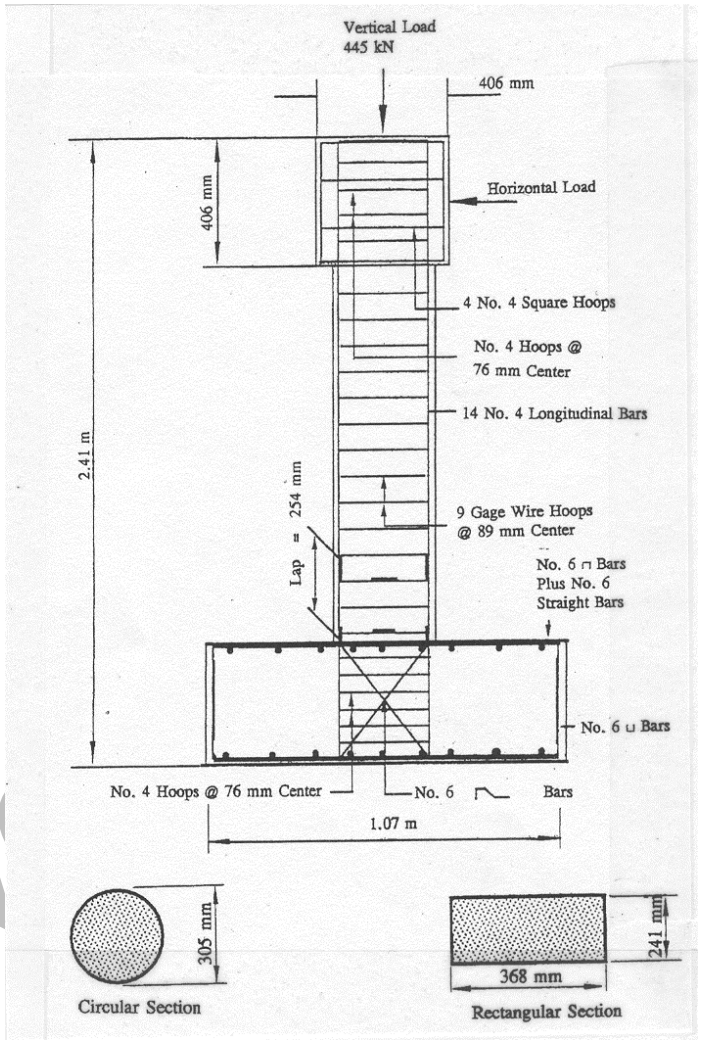

Fig. 3. Specimen details.

The plastic hinging region for some of the columns were confined by Fiber Reinforced Polymer (FRP) wraps. E-glass fibers in the form of a unidirectional fabric were used in the construction of the composite wraps. The fabrication of the composite wraps involved laying flat a long strip of 150-mm wide unidirectional E-glass fabric and saturating it with polyester resin matrix. A layer of mylar sheet was then placed on the wet strip, and then the strip was rolled around a mandrel representing the size and shape of the column cross section and placed in an oven to cure. The mylar sheet was provided to prevent bonding of the composite strip (wrap) to itself while curing. The wet composite wrap was cured at 71 °C for 40 minutes. Figure 4 shows some of the finished FRP wraps or straps ready to be used in the repair or retrofit of columns.


Fig. 4. FRP wraps (or straps) fabricated in the laboratory for the study.

The mechanical properties of FRP wraps were determined through tests conducted on specimens designed according to ASTM D3039-76. The data obtained from these tests were used to evaluate various

Archive

www.SID.ir

material parameters necessary for the analysis and design of test columns. As shown in Fig. 5, the stress-strain behavior of FRPs is linearly elastic to failure and depends on the fiber content. The fiber volume ratio shown in this figure is defined as the volume of fibers over the total volume of composite material. Three different fiber contents were tried for this study. A volume content of 50.2% was selected since it represents a fiber content that can be easily achieved in the field. Thus, the wraps were 0.8 mm thick and had a tensile strength of 532 MPa.

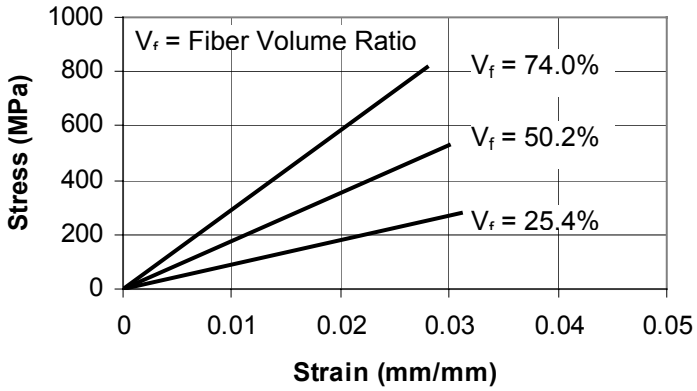

Fig. 5. Stress-strain behavior of E-glass FRPs.

Construction of Specimens

All column specimens were cast using a ready-mix concrete that was delivered to the laboratory. Four of the specimens (C1, C4, R1, and R3) were tested first without any retrofit; this was to establish a frame of reference for the performance of poorly detailed columns that exist in many older structures. These four columns were subsequently repaired by wrapping them in FRP straps and they were retested; these are referred to as "repaired" specimens and are designated as C1R, C4R, R1R, and R3R in Table 1. Six other specimens (C2, C3, C5, R2, R4, and R5) were strengthened with FRP jackets before they were tested. There are referred to as "retrofit" specimens.

In this study, FRP straps were fabricated in advance to fit the column cross sections. This was intended to simulate a scenario where the straps would be manufactured in a plant for better quality control and to minimize field operations. Nowadays, it is common to wrap the resin-saturated fabrics directly onto the column in the field and allow the FRP to cure at ambient temperature on site. Saturating machines are available that impregnate the fabric uniformly with resin and result in high quality FRP products.

Four bands of FRP were placed adjacent to each other covering approximately a 600-mm height of the column directly above the footing. The number of plies of FRP straps needed for repair or retrofit was calculated based on the required additional confinement pressure to bring the column to current design standards. Due to the small thickness, the cured straps were flexible enough to be wrapped around the columns (Fig. 6). As the FRP straps were wrapped around the column, an epoxy was applied to its surface and the multiple layers of the strap were adhered together to form a single composite wrap with the desired thickness. The epoxy was selected to insure that the multiple layers of FRP acted as one unit with no interlaminar slippage.

Some of the specimens were retrofit with passive confinement. In this case, the FRP is wrapped around the column. As the concrete in the column is damaged and dilates outward, its expansion is

Archive of SID

www.SID.ir

resisted by the FRP jacket. Thus, only beyond that point the FRP begins to apply a confining pressure to the column. Other specimens were repaired or retrofit using active confinement. In this case, the FRP straps are wrapped around the column and after the epoxy is cured, a resin is pressure injected into the gap between the FRP and concrete column (Fig. 6). This forces the resin into the micro cracks of the concrete and places the FRP in tension (similar to prestressing). During the initial stages of pressure injection, some of the epoxy would migrate up through the micro cracks and pores. Additional epoxy was injected to compensate for the loss of pressure due to this migration and to achieve a relative stable pressure. It is anticipated that this pressure could further drop with time as the epoxy migration would continue. Moreover, this pressure could further drop as a result of the creep of epoxy and the wrap. However, at these low levels of injection pressure, the contribution of the latter two to the loss of pressure was expected to be minimal.

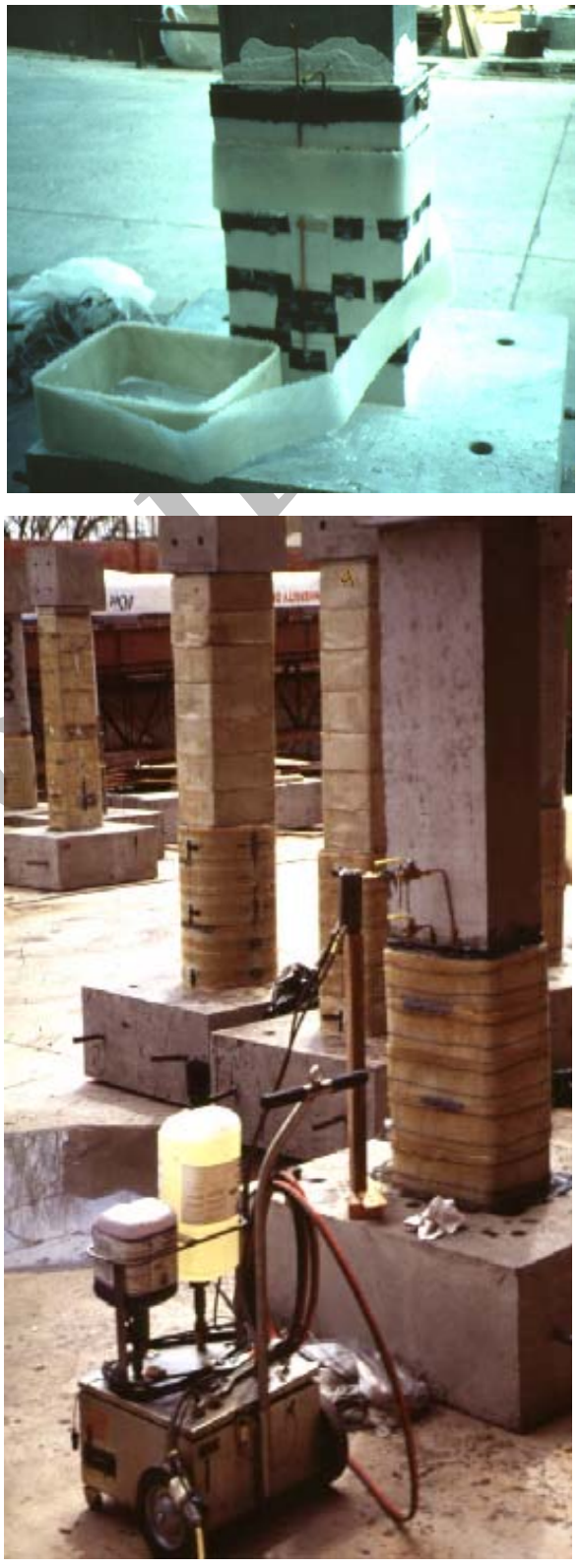

Fig. 6. Wrapping of FRP straps around columns and pressurizing for active confinement.

Test Setup and Loading

The specimens were tested in a steel reaction frame as show in Fig. 7. Two independent loading systems were used to apply the load to the specimens. The axial load of 445 kN was applied to the column by prestressing a pair of 25-mm diameter high-strength steel rods against the base of the test frame, which was bolted to the 900-mm thick concrete floor. This load was applied to simulate the vertical dead and live loads on the column. The magnitude of this load was determined based on the scale factor of 1/5 over the tributary area, resulting in a factor of 1/5 x 1/5 = 1/25. The prototype column had been designed for a gravity load of $0.15A_g f'_c$ or 11,200 kN, which is equivalent to an axial load of 445 kN on the test columns. While maintaining this axial load constant, lateral loads were applied to the top of the specimen.

The lateral loads were generated by an HP-

Archive of SID

www.SID.ir

computer controlled MTS ±490 kN hydraulic actuator mounted on the reaction frame. The actuator was capable of moving the top of the specimen 125 mm in both positive and negative directions. A displacement of 125 mm corresponds to a ratio of lateral displacement to column height of approximately 7%. The load and displacement input history was broken into two phases. In the first four cycles of loading, the actuator was operated in the load-controlled mode. The maximum load in each cycle was gradually increased to that corresponding to the yield load of the specimen during the fourth cycle. Beyond that point, the loading was changed to the displacement-controlled mode for the remainder of the test. The displacement ductility factor, u, is defined as the ratio of the maximum applied displacement in each cycle to that corresponding to the first yielding of longitudinal bars. Thus, in the remaining cycles, the specimens were subjected to cyclic displacements corresponding to u=1, 1.5, 2, 3, 4, and 5. Approximately 14 strain gages were attached to the reinforcing bars in the critical regions of the specimens. Additional strain gages were also mounted on the exterior layer of the FRP straps after they were wrapped around the columns. In addition, 5 clinometers were externally attached to the plastic hinging region of the columns to measure the rotation of the column along the height. More detailed information on the instrumentation of these specimens is given elsewhere [3-5].

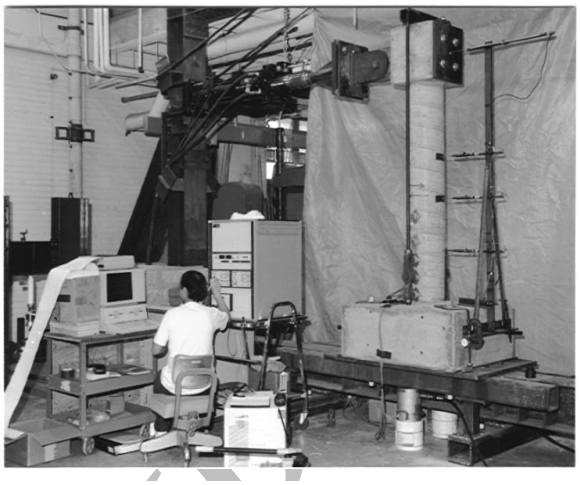

Fig. 7. Test setup.

Observed Response

Plots of the lateral load vs. displacement for Specimens C1 and C2 are shown in Fig. 8. Due to space limitation, the reader is invited to refer to other publications for data on remaining specimens [3-5]. Because the specimens were symmetrically reinforced, the resulting positive and negative portions of the hysteresis loops should be symmetrical and identical in value. However, due to a limitation in the hydraulic actuator, the maximum stroke reached in the positive and negative directions were slightly different for some of the test specimens. This difference affected the symmetries of the hysteresis loops. In Fig. 8, V_u is the lateral force corresponding to the theoretical flexural capacity of the unconfined concrete column section, δ_y is the yield displacement that was used as a reference value to determine the maximum displacement in each subsequent loading cycle. The measured and calculated maximum strength for all specimens are summarized in Table 1. The calculated strength was determined using the procedures outlined in the ACI Code [6] and taking into consideration the actual strain hardening properties of the reinforcing steel. The percent increase was calculated with reference to the measured value for the control specimen.

Figure 8 shows that the hysteretic response of the non-retrofit circular column with lap splice reinforcement (C1) degrades rapidly after the first cycle to u=1.5 due to bond failure of the lapped reinforcement. The maximum lateral load of 58.3 kN was recorded during the push cycle to u=1.5. Specimen C2 was identical to C1 but was wrapped with 6 layers of FRP. The response of this specimen was significantly improved compared to C1. The load resisted by the specimen increased

Archive of SID

www.SID.ir

with each cycle of loading through a displacement ductility of u=6 to 81.4 kN. This is 40% higher than the load carried by C1.

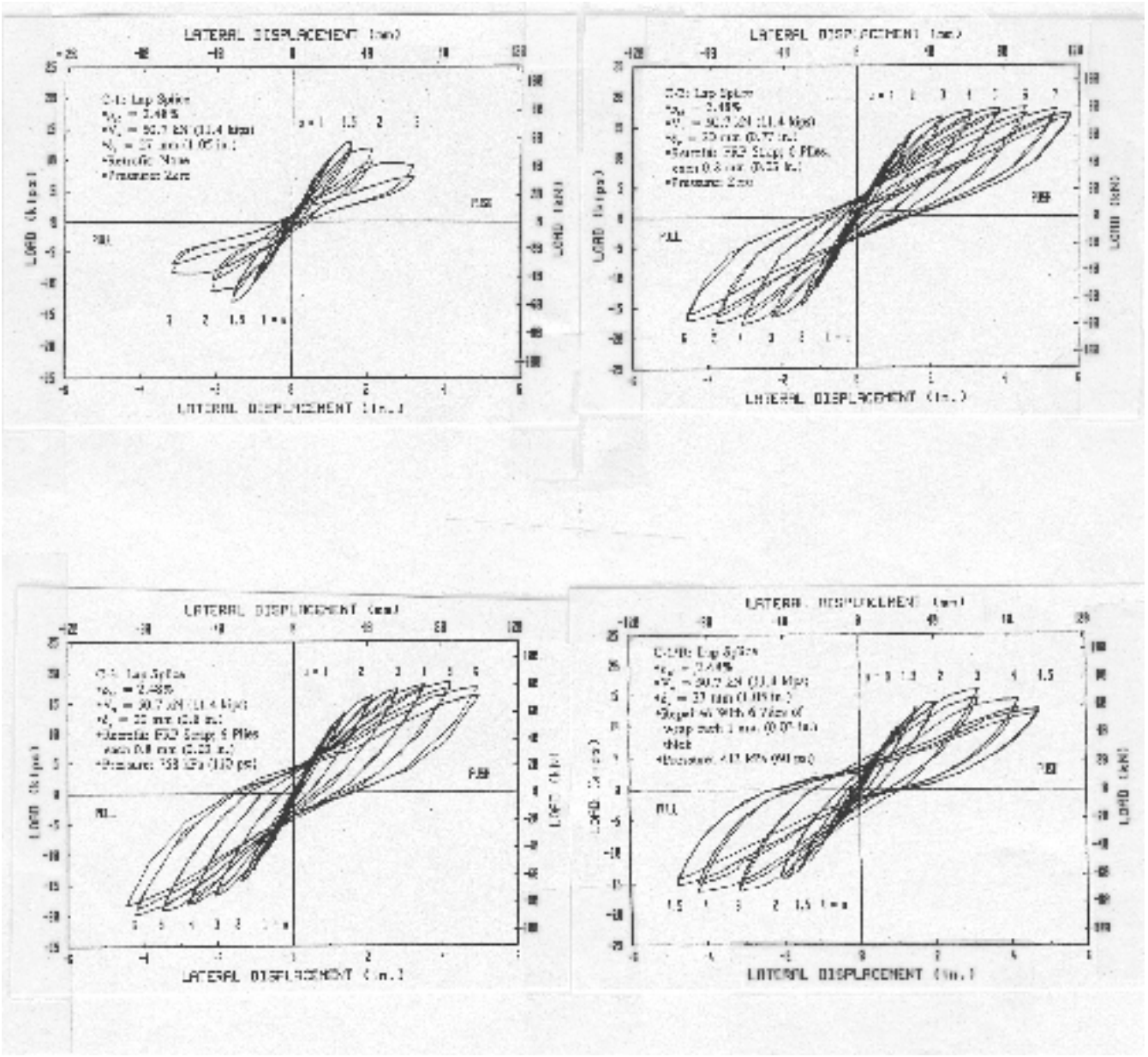

Fig. 8. Hysteretic response of Specimens C1, C2, C3, and C1R.

www.SID.ir

Specimen C3 was constructed identical to Specimens C1 and C2. It was retrofit by active confinement with injecting resin to a pressure of 758 kPa; its behavior was very similar to C2. The maximum load for this specimen was 89.4 kN or 53% higher than that of C1. This increase compared to C2 can be attributed to active confinement. Similar increases were realized for all circular and rectangular specimens and the results are summarized in Table 1.

Four of the original specimens (C1, C4, R1, and R3) were repaired following the original test and were retested. The repair consisted of replacing all loose and damaged concrete near the base of the column with new concrete and compacting it with hand. Due to access limitation, this concrete could not be adequately compacted. The plastic hinging regions of these columns were then wrapped with several layers of FRP and a resin was pressure-injected as discussed earlier. This ensured that any voids caused by poor compaction were filled. These repaired specimens were retested.

The hysteretic response of Specimen C1R is also shown in Fig. 8. The performance of the repaired specimens was far superior to that during the original test in terms of load capacity and ductility. At the displacement ductility level of u=3, where the original column had failed, no structural degradation was observed in the repaired column. In fact, the response of the repaired column had improved over the original, undamaged column (C1). The increase in load carrying capacity of the repaired columns compared to that measured during the original test is also listed in Table 1. This indicates that the behavior of the wrapped specimens is primarily a function of the confinement provided by the FRP jacket. The repaired specimens did, however, have slightly lower stiffness. This is attributed to the loss of bond between the steel and concrete and the formation of cracks in the specimens during the original test.

In general, confining jackets are more effective when they are placed around circular columns. For rectangular concrete sections, the effectiveness of the confinement diminishes as the sides of the column become larger. In this study, one of the rectangular columns (R5) was identical to R4 except that in the case of R5, the region near the base of the column was first enlarged into an oval shape using a fast-curing cement [4]. While the behavior of these two specimens was very similar, Specimen R5 carried about 8% more load; this increase can be attributed to the improved confinement provided by the oval jacket.

Analysis of the strain gage data also confirmed the improved behavior caused by the introduction of the FRP jackets. Generally, in non-retrofit columns, the longitudinal bars were less strained compared to retrofit columns. Factors contributing to this were the insufficient confinement, bond failure in the lapped starter bars, and/or buckling of continuous bars in non-retrofit columns. Confinement by composite straps allowed higher strains in longitudinal bars before failure, resulting in higher overall ductility and energy absorption capacity of the retrofit columns.

Insufficient confinement leads to premature yielding of the confining steel, loss of confinement and rapid deterioration of the plastic hinge region. In general, for a given level of displacement, strains in hoops of retrofit columns were significantly lower than those in non-retrofit specimens. Strain gage data also demonstrated that the FRP jackets were carrying significant tensile forces and were contributing to the confinement and reducing dilation of the core concrete.

Archive of SID

www.SID.ir

RETROFIT MODELING

The interaction diagram for a reinforced concrete column is qualitatively shown in Fig. 9 with a light line. For seismic regions, not only the strength, but also the deformability of the column is of great interest. Thus, the P-M diagram shown here also includes a companion curvature diagram. As can be seen, in regions of high axial load, the curvature at failure is fairly small. For tension failure (i.e. below the balanced axial load), the curvature is larger and increases as the axial load is reduced towards zero. When a column is retrofit, a new P-M-ϕ diagram results as qualitatively depicted with heavier lines in Fig. 9.

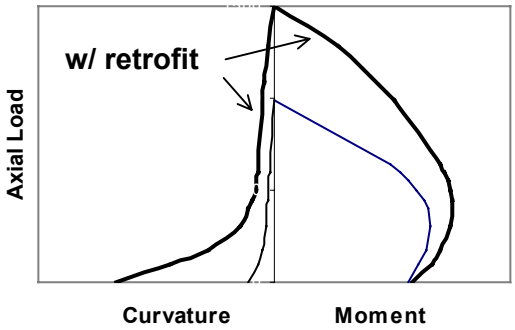

Fig. 9. Comparison of P-M-ϕ diagrams for R/C columns with and without retrofit.

The contribution of the external confinement to the columns has been modeled [7]. Due to space limitation the derivation of the model is discussed only briefly here. In this case, one must calculate the improved stress-strain behavior of concrete that is obtained as a result of external confinement, i.e. the graph shown with a thick line in Fig. 2. The principles of energy balance are utilized for this purpose. The additional strain energy stored in the concrete after yielding of the existing steel is equal to the strain energy of the composite wrap. This calculation is fairly cumbersome to be carried out by hand and lends itself well to a computer program. As the strain in the concrete is increased, it starts to dilate and expand outwards; this dilation results in increased tension in the external jacket, which in turn pushes more on the concrete (i.e. confines the concrete). This will continue until the jacket breaks in tension. The model also accounts for the lower efficiency of the confinement that exists when the column cross section is rectangular.

Once the stress-strain diagram for the confined concrete is determined, the points on a column interaction diagram can be calculated. For a given value of strain in the extreme fiber of concrete, the depth to the neutral axis can be assumed and the strains at any point on the cross section can be calculated assuming that strains vary linearly. From the strains, stresses in concrete and steel and the corresponding force in these elements can be calculated. The difference between the internal compression and tension resultants is the axial load acting on the column. The moments of the internal forces can also be calculated. Curvature of the section is calculated by dividing the maximum concrete strain by the depth to the neutral axis. This procedure can be repeated and each set of calculations leads to a set of points to be plotted on the P-M-ϕ diagram.

There are a couple of points regarding the interaction diagram of the retrofit columns that deserve special attention. First, because the fibers in the FRP jackets are oriented in the horizontal (i.e. hoop) direction, they do not increase the bending capacity of the column much. This is important because increase in the bending capacity of the column may make the column stronger than the footing, and in a potential future earthquake, the footing may fail. Due to access limitations, repair of footings is more difficult and less desirable than that of columns. The second advantage to note

Archive of SID

www.SID.ir

is the significant increase in ductility or curvature of the column. This is particularly true for regions of low axial loads that are more significant in practice. In fact, the primary interest in retrofit of most columns is to increase their ductility at low axial load levels with little increase in strength. Both of these objectives are readily achieved by use of FRP jackets.

In a typical retrofit scenario, analysis of the structure will identify the ductility demand on the column. That is, it will be demonstrated that the column of length L must be capable of maintaining its load while it is ends undergo a relative displacement, δ. The moment diagram for the column assuming that both ends are fixed is shown (Fig. 10). The deflection of the column can be calculated using the moment area theorem. The plastic hinging region of the column is spread over a distance L_P. Several researchers have suggested estimates for the calculation of the plastic hinge length and many of these have been summarized by Park and Paulay [8]. One recommendation sets this length approximately equal to (0.3) x (the diameter of the column bar) x (the yield strength of the longitudinal column bars). For practical purposes, one can assume that the plastic curvature (ϕ_P) remains constant over the plastic hinge region. The yield and plastic curvatures are obtained from the P-M-ϕ diagram of the retrofit column cross section as discussed above. The calculated deflection of the columns is checked against the anticipated displacement, δ. If the displacement is not large enough, additional layers of FRP wraps must be added to further increase the plastic curvature and deformability of the column.

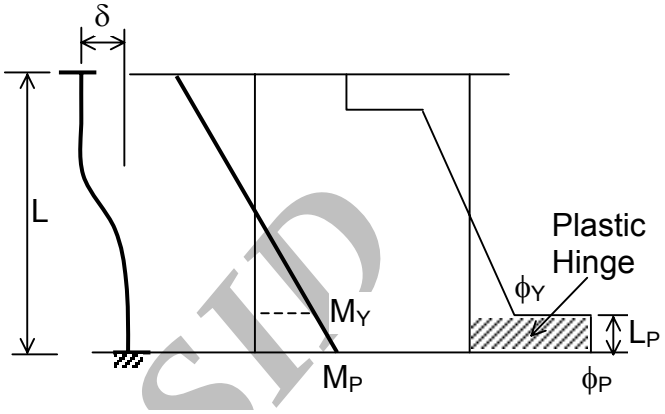

Fig. 10. Displacement, moment and curvature of retrofit column.

In case the column needs to be strengthened for flexure, FRP straps must be applied to the column surface such that the fibers in the FRP are placed parallel to the longitudinal bars in the column. However, for these to be fully effective in resisting moments they must be attached to the footing and the floors above; this type of connection cannot be easily detailed and further studies on this subject are needed.

Wrapping the entire height of the column with FRP straps with the fibers oriented in the horizontal direction can also provide shear enhancement for the column. In the case of shear strengthening, it is recommended to limit the strain in the FRP to 0.004. This ensures that the sear cracks do not widen too much and that aggregate interlock remains a contributing factor to the overall shear resistance mechanism.

SUMMARY AND CONCLUSIONS

This paper has summarized some of the recent investigations in repair and retrofit of reinforced concrete columns with fiber composites. Results from tests of 14 columns have been introduced. It is concluded that FRPs can be effectively used to significantly increase the strength and ductility of

Archive of SID

www.SID.ir

poorly detailed columns. While most columns constructed prior to mid 1970s fail after a couple of cycles at low ductility ratios, columns retrofit with FRPs can withstand multiples of cycles of loading to displacement ductility levels of six or beyond, without loss of strength. Similar behavior was observed for columns that were damaged as a result of an initial loading and were subsequently repaired and retested. The confinement provided by the FRPs reduces the dilation of the concrete and improves the bond between the reinforcing steel and concrete; this leads to a more ductile response of the structure. The procedure for calculating the behavior of retrofit columns was also introduced. These steps can guide the engineer to calculate the required thickness of FRP to ensure a certain level of deformability for the column.

REFERENCES

1. Priestly, M.J.N., Seible, F., Chai, Y.H., and Sun, Z. (1998). "Steel Jacketing of Bridge Columns for Enhanced Flexural Performance," *Proceedings*, NSF Symposium on Bridge Research in Progress, Des Moines, Iowa, pp. 205-208.

2. Mei, H., Kiousis, P.D., Ehsani, M.R., and Saadatmanesh, H. (2001). "Confinement Effects on High Strength Concrete," *ACI Structural J., 98(4), 548-553.*

3. Saadatmanesh, H., Ehsani, M.R., and Jin, L. (1996). "Seismic Strengthening of Circular Bridge Pier Models with Fiber Composites," *ACI Structural J., 93(6), 639-647.*

4. Saadatmanesh, H., Ehsani, M.R., and Jin, L. (1997). "Seismic Retrofitting of Rectangular Bridge Columns with Composite Straps," *Earthquake Spectra, 13(2), 281-304.*

5. Saadatmanesh, H., Ehsani, M.R., and Jin, L. (1997). "Repair of Earthquake-Damaged R/C Columns with FRP Wraps," *ACI Structural J., 94(2), 206-215.*

6. ACI Committee 318. (1989). "Building Code requirements for Reinforced Concrete and Commentary (ACI 318M-89/ACI 318RM-89)," American Concrete Institute, 351 pp.

7. Saadatmanesh, H., Ehsani, M.R. and Li, M.W. (1994). "Strength and Ductility of Concrete Columns Externally Reinforced with Fiber Composite Straps," *ACI Structural J.*, 91(4), 434-447.

8. Park, R., and Paulay, T. (1975). "Reinforced Concrete Structures," John Wiley and Sons, New York, 769 pp.

Archive of SID

www.SID.ir

Surf and download all data from SID.ir: www.SID.ir

Translate via STRS.ir: www.STRS.ir

Follow our scientific posts via our Blog: www.sid.ir/blog

Use our educational service (Courses, Workshops, Videos and etc.) via Workshop: www.sid.ir/workshop